Inductive source induced polarization

David Marchant*, Eldad Haber and Douglas W. Oldenburg, University of British Columbia

SUMMARY

We propose a new methodology for processing frequency domain EM data to identify the presence of IP effects in observations of the magnetic fields arising from an inductive source. The method makes used of the asymptotic behaviour of the imaginary part of secondary magnetic fields at low frequency. A new quantity, referred to as the ISIP datum, is defined so that it equals zero at low frequencies for any frequency-independent (non-chargeable) conductivity distribution. Thus any non-zero response in the ISIP data indicates the presence of chargeable material. Once the data are defined, the change in the real component of the resistivity, which is indicative of chargeability, is obtained by solving a linear inverse problem.

INTRODUCTION

Induced polarization (IP) surveying is often the geophysical method of choice when exploring for disseminated sulphides. The IP method maps the distribution of chargeability in the subsurface which has been shown to be an excellent proxy for metallic mineralization (Fink et al., 1990).

A number of physical mechanisms cause chargeability in a material (Fuller and Ward, 1970). Fundamentally, a chargeable material is one that possesses a complex, frequency dependent resistivity. This frequency dependence is commonly described by the Cole-Cole model (Pelton et al., 1978)

$$\rho\left(\omega\right) = \rho_0 \left(1 - \eta \left(1 - \frac{1}{1+(i\omega\tau)^c}\right)\right) \qquad (1)$$

In this expression, ρ_0 is the resistivity (Ωm) at zero frequency, η is the chargeability, τ is a time constant (seconds), and c is the frequency dependence. The chargeability has a value between 0 and 1. It determines the magnitude of the difference in the resistivity between the low and high frequency asymptotes. The value of the time constant determines the frequency at which the magnitude of the imaginary resistivity peaks. The frequency dependence controls the sharpness of the transition between the two asymptotic values.

Traditionally, chargeability is mapped using the IP method (Seigel, 1959) in either the time or frequency domain. In this technique, currents are injected into the ground through a pair of transmitter electrodes while measurements are made at a different pair of receiver electrodes. In the time domain, a constant current is injected until a steady state is reached. The current is then interrupted, and the resulting voltage decay is measured across at the receivers. In the frequency domain, a sinusoidally varying current is injected at differences, and the change in voltage and/or phase shift is recorded. Another method used is the magnetic induced polarization (MIP) technique (Seigel, 1974). In this technique, current is again in-

jected into the ground across two transmit electrodes, but observations of the secondary magnetic field are used rather than electrical potentials. This eliminates the time consuming requirement of placing receiver electrodes, and provides improved performance when operating where highly conductive overburden exists. Inversion routines have been developed to invert these data in two or three dimensions (Oldenburg and Li (1994), Li and Oldenburg (2000), Chen and Oldenburg (2003)).

The IP and MIP methods are widely applied throughout the mining industry and have been very successful exploration tools. Despite their success, their application is not always practical. The time and cost required to survey large areas can be prohibitively large. Some geologic settings can also cause traditional IP or MIP to fail. For example, when high resistivity is present it becomes difficult to inject enough current into the ground to excite the polarizable body.

In order to avoid having to inject current into the ground, one must move to a purely inductive method. The idea of inductive induced electrical polarization was examined by Hohmann et al. (1970). They considered frequency-domain measurements acquired above a 1D, chargeable 2-layer model as well as field data collected above known conventional IP responses. They considered only the magnitude of the magnetic field as data. In the synthetic tests, while the presence of a chargeable layer did affect the data, the changes were very small. Although such changes could be explained in terms of chargeable material it seemed that a heterogeneous model with frequency independent conductivity could provide another possible explanation. Numerous other studies have been published regarding the effects of chargeability on inductive EM, but the vast majority of those focus on presence of negative transients in concentric and in-loop TEM surveys. In this work, we propose a new data collection and processing methodology to map the distribution of chargeability using inductive sources and observations of magnetic fields in the frequency domain. We exploit the asymptotic behaviour of the magnetic fields at low frequencies to identify the presence of an IP response.

THEORY

Maxwell's equations in the frequency domain are

$$\nabla \times \mathbf{E} + i\omega\mu\mathbf{H} = 0 \qquad (2)$$
$$\nabla \times \mathbf{H} - \sigma\mathbf{E} = \mathbf{s}$$

Here, $\mathbf{E}$ and $\mathbf{H}$ are the electric and magnetic fields, σ is the conductivity and μ the magnetic susceptibility. Separating $\mathbf{H}$ into $\mathbf{H} = \mathbf{H}_0 + \mathbf{H}^s$ and eliminating $\mathbf{E}$ from this systems yields

$$\nabla \times \rho\nabla \times \mathbf{H}^s - i\omega\mu\mathbf{H}^s = i\omega\mu\mathbf{H}_0 \qquad (3)$$

where $\mathbf{H}_0$ is defined to be the zero-frequency response of the source and ρ is the resistivity, $\rho = \frac{1}{\sigma}$.

Inductive source induced polarization

We will focus on using low frequencies for our experiment. By performing a Taylor series expansion of $\mathbf{H}^s$ about $\omega = 0$ and dropping the higher order terms we obtain

$$\mathbf{H}^s(\omega) \approx \frac{\partial \mathbf{H}^s}{\partial \omega}\bigg|_{\omega=0} \omega + \frac{1}{2}\frac{\partial^2 \mathbf{H}^s}{\partial \omega^2}\bigg|_{\omega=0} \omega^2 \qquad (4)$$

Assume we are working with material that is not chargeable (a frequency independent ρ). We can then compute the derivatives of $\mathbf{H}^s$ with respect to ω by differentiating equation 3. Differentiating, and evaluating the results at $\omega = 0$ gives

$$\nabla \times \rho \nabla \times \frac{\partial \mathbf{H}^s}{\partial \omega} = i\mu \mathbf{H}_0 \qquad (5)$$

The operator $\nabla \times \rho \nabla \times$ is purely a real, as are the fields $\mathbf{H}_0$. Using equation 5, we can see that $\frac{\partial \mathbf{H}^s}{\partial \omega}$ evaluated at $\omega = 0$ is an imaginary quantity. Thus

$$\mathsf{Im}(\mathbf{H}^s(\omega, \rho)) \approx \frac{\partial \mathbf{H}^s}{\partial \omega}\bigg|_{\omega=0} \omega \qquad (6)$$

Or

$$\frac{\mathsf{Im}(\mathbf{H}^s(\omega, \rho))}{\omega} \approx \frac{\partial \mathbf{H}^s}{\partial \omega}\bigg|_{\omega=0} \approx const. \qquad (7)$$

The value of this constant will depend on the geometry of the transmitter and receiver and the resistivity distribution in the ground. We demonstrate this in Figure 1 which shows $\frac{\mathsf{Im}(\mathbf{H}^s_z(\omega, \rho))}{\omega}$ observed at a single receiver for a range of frequencies. The simulation is carried out above a 3D resistivity distribution used for our synthetic example later in this paper.
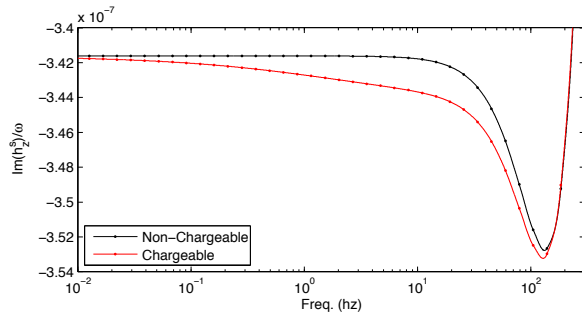

Figure 1: $\frac{\mathsf{Im}(\mathbf{H}^s_z(\omega, \rho))}{\omega}$ observed at a single receiver for a range of frequencies. Simulation is carried out above a 3D resistivity distribution with zero chargeability (black) and a 3D resistivity distribution containing chargeable materials (red). The quantity is constant at low frequency when no chargeable materials are present.

Inductive source induced polarization

Consider the magnetic response of a non-chargeable earth to forcing from an inductive source operating at two closely spaced, low frequencies ω_1 and ω_2. If the frequencies are sufficiently low then the skin-depth is very large compared to the geometric decay of the source fields. Therefore, the responses at the two frequencies should be predicted by the same conductivity distribution. From equation 7 we can say that

$$\frac{\mathsf{Im}(\mathbf{H}^s(\omega_2))}{\omega_2} - \frac{\mathsf{Im}(\mathbf{H}^s(\omega_1))}{\omega_1} \approx 0 \qquad (8)$$

This observation motivates us to define the new quantity d^{Im} which we define as the Inductive Source IP (ISIP) data.

$$d^{\mathsf{Im}} = \mathsf{Im}(\mathbf{H}^s(\omega_2)) - \frac{\omega_2}{\omega_1}\mathsf{Im}(\mathbf{H}^s(\omega_1)) \qquad (9)$$

A synthetic example

The ISIP data's sensitivity to chargeable material will be demonstrated using a synthetic example. The model consists of two conductive blocks buried in a complicated 3D background beneath a very resistive overburden. The zero-frequency resistivity of the blocks is $1\Omega m$, the background varies from $10\Omega m$ to $1000\Omega m$, and the overburden is $10000\Omega m$. Block #2 has Cole-Cole parameters of $\eta = 0.1$, $\tau = 0.1$ and $c = 0.5$. The rest of the model has $\eta = 0$. Two slices of the distribution of ρ_0 are shown in Figure 2(b) and 2(c)

The response from a single, 100m on a side transmitter loop is simulated. It's location relative to the blocks in the model is shown in Figure 2(a). The transmitter is simulated operating at 1hz and 2hz. The vertical component of the resulting secondary magnetic fields at each frequency are shown in Figures 3(a) and 3(b). The observed fields appear to be very similar and individually don't show any indication of an IP response. The calculated ISIP data are shown in Figure 3(c). The approximate location of the chargeable block is clear. The conductive block that had zero chargeability produces no ISIP response.

Sensitivity analysis

Chargeability causes small perturbations in resistivity as a function of frequency. Let ρ_1 and ρ_2 be the resistivities that would be observed at frequencies ω_1 and ω_2. The frequencies ω_1 and ω_2 are closely spaced, so the resistivity that would be observed at ω_2 is equal to the resistivity at ω_1, plus a small perturbation, or $\rho_2 = \rho_1 + \Delta\rho$. Expanding the magnetic field using the first order Taylor's expansion we obtain

$$\mathbf{H}^s(\omega_2, \rho_2) \approx \mathbf{H}^s(\omega_2, \rho_1) + \frac{\partial \mathbf{H}^s}{\partial \rho}(\omega_2, \rho_1)\delta\rho \qquad (10)$$

Define the complex sensitivity matrix $\mathbf{J}$ to be

$$\mathbf{J} = \frac{\partial \mathbf{H^s}}{\partial \rho}(\omega_2, \rho_1) \qquad (11)$$

Using the result from equation 7 we can say that

$$\mathsf{Im}(\mathbf{H}^s(\omega_2, \rho_1)) \approx \frac{\omega_2}{\omega_1}\mathsf{Im}(\mathbf{H}^s(\omega_1, \rho_1)) \qquad (12)$$

Substituting these expressions into equation 10 yields

$$\mathsf{Im}(\mathbf{H}^s(\omega_2, \rho_2)) \approx \frac{\omega_2}{\omega_1}\mathsf{Im}(\mathbf{H}^s(\omega_1, \rho_1)) + \mathsf{Im}(\mathbf{J}\delta\rho) \qquad (13)$$

Then, using the definition of the ISIP data (equation 9) we obtain

$$d^{\mathsf{Im}} = \mathsf{Im}(\mathbf{J}\delta\rho) = \mathbf{J}_{\mathsf{Re}}\delta\rho_{\mathsf{Im}} + \mathbf{J}_{\mathsf{Im}}\delta\rho_{\mathsf{Re}}. \qquad (14)$$

where we use the notation $(\cdot)_{\mathsf{Re}}$ and $(\cdot)_{\mathsf{Im}}$ to denote the real and imaginary components of $\mathbf{J}$ or $\delta\rho$. At low frequency, $||\mathbf{J}_{\mathsf{Re}}|| \ll ||\mathbf{J}_{\mathsf{Im}}||$ so

$$d^{\mathsf{Im}} \approx \mathbf{J}_{\mathsf{Im}}\delta\rho_{\mathsf{Re}} \qquad (15)$$
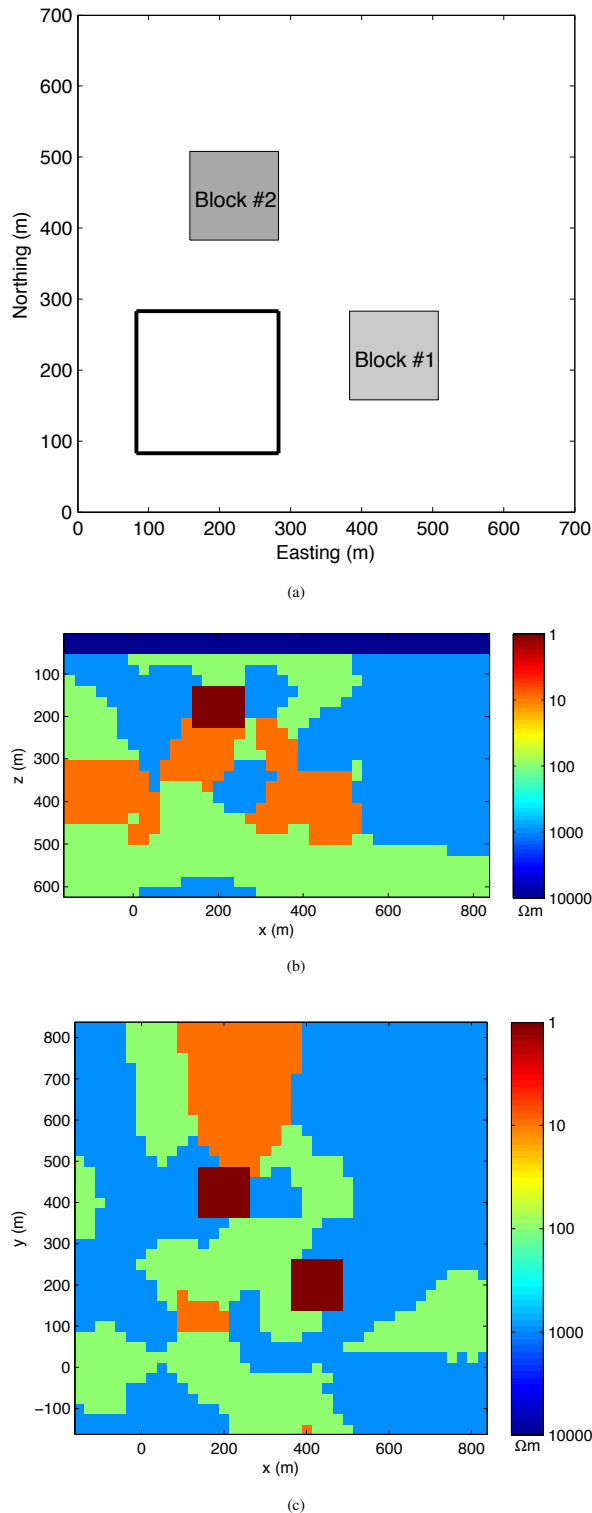
Figure 2: (a) Transmitter geometry of the synthetic example. The dark black line represents the transmitter wire. (b) Cross-section through the zero-frequency resistivity model at y = 400m. (c) Plan view of the zero-frequency resistivity model at z = The North-West conductive block also possess a non-zero chargeability.

CONSIDERATIONS

Dispersion spectra and selection of frequencies

Equation 15 tells us that the magnitude of the ISIP data is proportional to the change in the real portion of the resistivity between the two frequencies. When $c = 1$, the dispersion is limited to a narrow band of frequencies, the location of which is determined by the value of τ. Depending on the values of τ, ω_1, and ω_2 the values of the ISIP data may be much smaller, or equal to zero. As the value of c decreases, the transition from the low to the high asymptotes becomes broader. This makes the choice of ω_1 and ω_2 less important, but also results in smaller ρ_{Re} and thus a smaller magnitude ISIP response.

Noise

As we can see in Figure 3(c), the signals we are interested in are small, and thus they will be sensitive to errors in the measurement of the magnetic fields. If we assume that the errors in $\mathsf{Im}\left(\mathbf{H}^s(\omega_1)\right)$ and $\mathsf{Im}\left(\mathbf{H}^s(\omega_2)\right)$ have a covariance of zero, then the uncertainty in the computed ISIP data would be

$$\sigma_{ISIP} = \sqrt{\sigma_{h_2}^2 + \left(\frac{\omega_2}{\omega_1}\right)^2 \sigma_{h_1}^2} \qquad (16)$$

where σ_{h_1} and σ_{h_2} are the uncertainties of $\mathsf{Im}\left(\mathbf{H}^s(\omega_1)\right)$ and $\mathsf{Im}\left(\mathbf{H}^s(\omega_2)\right)$ respectively.

The uncertainty in an ISIP datum will always be greater than the uncertainty in either of the measured magnetic fields. Thus, it is critical that the magnetic fields be measured as accurately as possible.

In the example shown in Figure 3, the uncertainty in the magnetic field measurements must be less than $2.33 \times 10^{-9} A/m$, or $2.9 fT$ in order or achieve a signal to noise ratio better than 1. This assumes that 1A is being transmitted at each of the frequencies. However, the magnitude of the ISIP response will depend on the EM-coupling between the transmitter, the receivers, and the chargeable body, and it will scale with the magnitude of the transmitter current. If both the transmitter and the receiver are placed directly above the chargeable block, and we assume that a transmitter current of 10A is possible at each frequency, then the allowable noise increases to $173.22 \times 10^{-9} A/m$, or $217.67 fT$. It may be possible to further improve these values through stacking ISIP data calculated from different pairs of frequencies, or by considering the total magnetic field.

INVERSION

Using equation 15 it is possible to formulate a linear inversion problem enabling the three-dimensional distribution of $\delta\rho_{Re}$ to be recovered. The inverse methodology follows the IP inversion that is described in (Li and Oldenburg, 2000). As in the IP case, the inversion of ISIP data requires the distribution of ρ_0 to form the sensitivity matrix. This can be estimated by first inverting the available field data to generate a 3D resistivity frequency independent distribution.

The response of the model shown in figure 2 was calculated for a survey consisting of 25 transmitters laid out in a 5 by
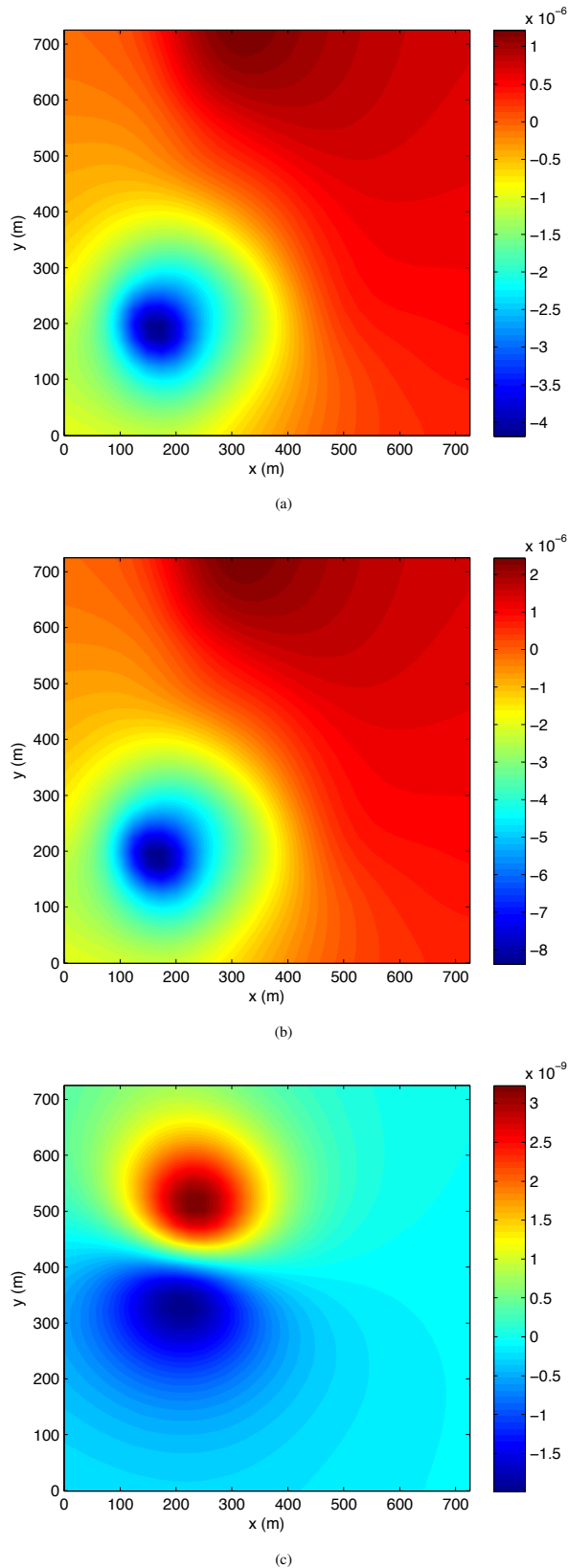
(a)

(b)

(c)

Figure 3: (a) Imaginary part of the vertical component of $\mathbf{H}^s$ observed at 1hz. (b) Imaginary part of the vertical component of $\mathbf{H}^s$ observed at 2hz. (c) Calculated ISIP data.

5 grid. Each transmitter was a square loop, 200m on a side. 225 receivers (15 by 15 grid) recorded the three components of the magnetic fields at 1hz and 2hz. Three components of ISIP data were then calculated from the simulated magnetic fields using equation 9, and were contaminated with synthetic noise. The 3D inverse problem was solved to recover $\delta\rho_{\mathrm{Re}}$. The chargeable material, coinciding with Block 2 in Figure 2(a) is shown in Figure 4.
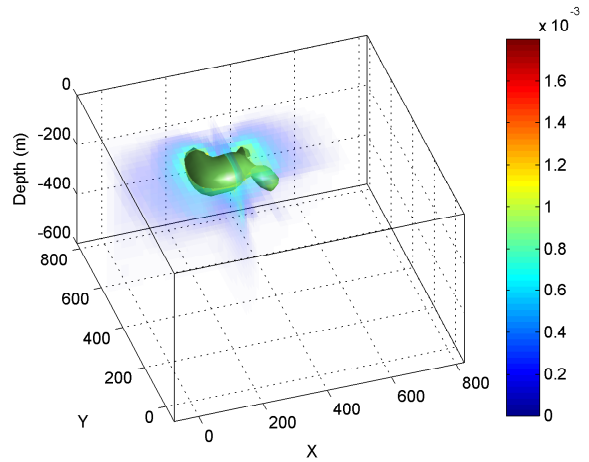

Figure 4: Recovered $\delta\rho_{\mathrm{Re}}$ for the synthetic inversion.

CONCLUSIONS

We have introduced a new methodology to detect chargeability using inductive magnetic sources. The method is based on the understanding that the low frequency response of the magnetic field to an inductive source is mainly imaginary. Using the simple asymptotic behaviour of the fields at low frequencies we introduce new data, that we refer to as the ISIP data. At low frequencies these data are identically zero if the conductivity is purely real. Thus any nonzero value of this datum is a direct indicator of chargeable material. Numerical simulations demonstrate that this is true even in a complex geological environment. Once ISIP data have been extracted, they can be inverted to reveal the real part of the resistivity change that arises from a chargeable earth. ISIP signals are small but should be measureable with modern instrumentation. If so, our technique could be used in many geological scenarios where measuring common IP data is difficult. Such scenarios include caliche covered environments and permafrost.

EDITED REFERENCES
Note: This reference list is a copy-edited version of the reference list submitted by the author. Reference lists for the 2012 SEG Technical Program Expanded Abstracts have been copy edited so that references provided with the online metadata for each paper will achieve a high degree of linking to cited sources that appear on the Web.

REFERENCES

Chen, J., and D. W. Oldenburg, 2003, 3-D inversion of magnetic induced polarization data: 16th Geophysical Conference, Australian SEG, Extended Abstracts, 1–11.

Fink, J. B., E. O. McAlister, B. K. Sternberg, W. G. Wieduwilt, and S. H. Ward, 1990, Induced polarization: Applications and case histories: SEG.

Fuller, B., and S. Ward, 1970, Linear system description of the electrical parameters of rocks: IEEE Transactions on Geoscience Electronics, **8**, 7–18.

Hohmann, G. W., P. R. Kintzinger, G. D. V. Voorhis, and S. H. Ward, 1970, Evaluation of the measurement of induced electrical polarization with an inductive system: Geophysics, **35**, 901–915.

Li, Y., and D. W. Oldenburg, 2000, 3-D inversion of induced polarization data: Geophysics, **65**, 1931–1945.

Oldenburg, D. W., and Y. Li, 1994, Inversion of induced polarization data: Geophysics, **59**, 1327–1341.

Pelton, W. H., S. H. Ward, P. G. Hallof, W. R. Sill, and P. H. Nelson, 1978, Mineral discrimination and removal of inductive coupling with multifrequency IP: Geophysics, **43**, 588–609.

Seigel, H. O., 1959, Mathematical formulation and type curves for induced polarization: Geophysics, **24**, 547–565.

Seigel, H. O., 1974, The magnetic induced polarization (MIP) method: Geophysics, **39**, 321–339.